EUKARYOTIC CELL, Mar. 2011, p. 302–312 Vol. 10, No. 3
1535-9778/11/$12.00 doi:10.1128/EC.00201-10

The Fungal Type II Myosin in *Penicillium marneffei*, MyoB, Is Essential for Chitin Deposition at Nascent Septation Sites but Not Actin Localization▽†

David Cánovas,#‡ Kylie J. Boyce,# and Alex Andrianopoulos*

Department of Genetics, University of Melbourne, Victoria 3010, Australia

Received 17 August 2010/Accepted 24 November 2010

Cytokinesis is essential for proliferative growth but also plays equally important roles during morphogenesis and development. The human pathogen *Penicillium marneffei* is capable of dimorphic switching in response to temperature, growing in a multicellular filamentous hyphal form at 25°C and in a unicellular yeast form at 37°C. *P. marneffei* also undergoes asexual development at 25°C to produce multicellular differentiated conidiophores. Thus, *P. marneffe*i exhibits cell division with and without cytokinesis and division by budding and fission, depending on the cell type. The type II myosin gene, *myoB*, from *P. marneffei* plays important roles in the morphogenesis of these cell types. Deletion of *myoB* leads to chitin deposition defects at sites of cell division without perturbing actin localization. In addition to aberrant hyphal cells, distinct conidiophore cell types are lacking due to malformed septa and nuclear division defects. At 37°C, deletion of *myoB* prevents uninucleate yeast cell formation, instead producing long filaments resembling hyphae at 25°C. The Δ*myoB* cells also often lyse due to defects in cell wall biogenesis. Thus, MyoB is essential for correct morphogenesis of all cell types regardless of division mode (budding or fission) and defines differences between the different types of growth.

Cellular division is a complex process required by all organisms for growth and differentiation. Cytokinesis and subsequent cell separation are either partially or completely dependent on the formation of an actomyosin contractile ring, depending on the particular organism. Actin and myosin are the major ring components and are supported by at least 130 other factors involved in cytokinesis (42). Cytokinesis and cell separation in both fission and budding yeasts occur in an analogous manner, despite key differences between these organisms. In the budding yeast *Saccharomyces cerevisiae*, the site of division is established either adjacent to or across from a previous division site during G_1 of the cell cycle (30). The Rho GTPase Cdc42p is recruited to the presumptive site of division, where it is activated and recruits the septin scaffold proteins in late G_1 (55). The sole type II myosin in *S. cerevisiae*, encoded by *MYO1*, is essential for actomyosin ring formation and is the first component of the ring to be assembled in a septin-dependent manner (7, 30, 50). At the end of anaphase, F-actin forms a ring in association with Myo1p. The actomyosin ring contracts and results in the invagination of the plasma membrane at the neck between the mother and daughter cells. The actomyosin ring eventually disappears, and the cells are separated initially by a primary septum and then by flanking secondary septa made of chitin (7). The cells separate after degradation of the primary septum, completing cytokinesis (43).

In the fission yeast *Schizosaccharomyces pombe*, the localization of the division site is selected before entry into mitosis (27). Fission yeasts position the nascent septum at the cell midpoint using an interphase negative signal from a concentration gradient of the kinase Pom1p, which concentrates at both poles (1, 33, 38), and the nucleus as a positional determinant, a process involving counterbalancing microtubule forces (16, 51). Localization of Myo2p depends on phosphorylation in the C-terminal coiled coil and occurs in a septation initiation network (SIN)-dependent manner (39). Cdc15p, the formin Cdc12p, ring assembly protein 2 Rng2p, and Mid1p simultaneously localize with Myo2p at the cytokinesis nodes (assemblies serving as the precursors of the contractile ring). The Rho GTPase Rho1p then regulates the formation of the ring through the activation of formins (55). F-actin cables form at neighboring nodes, and Myo2p captures the actin filaments, applying force to bring the nodes together. By pulling the neighboring actin filaments, myosin proteins assemble and constrict the ring (42). Unlike in *S. cerevisiae*, the motor domain of *S. pombe* type II myosins is required for cytokinesis (31).

In contrast to yeast and animal cells, filamentous fungi undergo cytokinesis without cell separation during proliferative growth. This process is termed septation and results in the separation of hyphal cells by the formation of chitin-rich structures (septa) composed of several electron-dense layers that are perforated by a single pore (36). This enables growth as multicellular compartmentalized hyphae. In *Aspergillus nidulans*, the duplication cycle is initiated by waves of nuclear division that extend basally from the tips of apical cells, and this mitotic wave is followed by septum formation in the apical cell (14, 26). Septation involves assembly of an actin ring between nuclei. Actin condensation and invagination initiation are closely followed by chitin synthesis at the edge of the invaginating actin ring. Actin withdraws from the developing

* Corresponding author. Mailing address: Department of Genetics, University of Melbourne, Victoria 3010, Australia. Phone: 61 3 8344 5164. Fax: 61 3 8344 5139. E-mail: alex.a@unimelb.edu.au.

† Supplemental material for this article may be found at http://ec.asm.org/.

‡ Present address: Departamento de Genética, Facultad de Biología, Universidad de Sevilla, Seville, Spain.

# These authors contributed equally.

▽ Published ahead of print on 3 December 2010.

septum in a punctuate form and eventually disappears, leaving the septal cell wall (36). Similar to that in *S. cerevisiae* and *S. pombe*, *A. nidulans* septum formation is actin dependent (19). However, in contrast to the case in these yeasts, actin localizes simultaneously at the tips of growing cells and at the site of septum formation (10, 19). In addition, microtubules are also required for the initiation and progression of septation (36).

Penicillium marneffei is a thermally dimorphic fungal pathogen which uses three different modes of division during the various stages of its life cycle (3). At 25°C, it grows in a multinucleate, branched, septate hyphal form by apical extension in a mode similar to that of most other filamentous fungi. Under the appropriate environmental conditions, hyphal cells undergo asexual development to produce conidiophores. The differentiated cell types present in the conidiophore emerge from a stalk cell by a sequential budding process which requires coupling of nuclear division and cell division. Cell separation is required to liberate the uninucleate asexual spores (conidia) from the terminal end of the differentiated conidiophore. At 37°C, *P. marneffei* undergoes a process termed arthroconidiation, where cellular division and nuclear division become coupled, hyphae lay down double septa, and cells subsequently separate to liberate uninucleate yeast cells. The yeast cells proliferate vegetatively by fission division. The capacity for three modes of cellular division in a single organism provides a unique system in which to probe the similarities and differences between these processes. Previous studies with *P. marneffei* have shown specialization in the control of these different modes of division by three small GTPase-encoding genes, with concomitant overlapping roles during cytokinesis (9–11). Therefore, *P. marneffei* is an excellent organism in which to compare the differences and similarities between the three modes of cellular division exhibited by fungi and whether the formation of an actomyosin ring is required for completion of cytokinesis in the different modes of division. Here we describe the cloning and characterization of a gene (*myoB*) encoding a type II myosin from *P. marneffei* and investigate its role in cytokinesis during the three modes of cellular division (hyphal growth, conidiation, and yeast morphogenesis).

MATERIALS AND METHODS

Molecular techniques. Genomic DNA was isolated as previously described (8). RNA was prepared by using the FastRNA red kit (BIO101). DNA-mediated transformation of *P. marneffei* has been previously described (8, 40). Reverse transcriptase PCR (RT-PCR) was performed by using SuperScript one-step RT-PCR with Platinum *Taq* (Invitrogen).

Cloning and plasmid construction. A primary clone of a myosin was obtained by PCR using degenerate primers MYO1 (5′-GGCGAGTCCGGCGCNGGNA ARAC-3′) and MYO2 (5′-CGTTGGCGTAGTTGATGCAGADYTGYTCRA A-3′) directed to the motor domain and based on the CODEHOP protocol (45). Sequencing confirmed the cloning of a type II myosin-encoding gene. This PCR product was used to map the genomic locus by Southern blot analysis and as a probe to hybridize to a genomic DNA library constructed in λBlueSTAR (Novagen). A single clone of 5.8 kb was obtained, containing the 5′ end of the gene and spanning the ATG start codon and the promoter (plasmid p4699). Based on the genomic map, inverse PCR was used to clone the rest of the gene as follows. Genomic DNA was digested with EcoRI and then self-ligated and used as a template for PCR with the divergent primers *myoB*_inv_low (5′-GGTGGAAG TCATACGGTCG-3′) and *myoB*_for (5′-AAACGCCCAGACAGTGAGG-3′). The resulting PCR product was digested with different combinations of restriction enzymes and cloned into pBluescript II SK(−) (Stratagene), which was previously digested with the appropriate restriction enzymes.

The Δ*myoB* deletion construct was generated by cloning an EcoRI/SmaI fragment containing the region upstream of the ATG of *myoB* from plasmid p4699 into the *pyrG* Blaster cassette plasmid pAB4626 (8) digested with EcoRI/EcoRV. The resulting plasmid was digested with XbaI/SmaI and ligated to a PCR product obtained from plasmid pDAP29 using primers M13 −21 and M13 reverse. Plasmid pDAP29 contained an EcoRI/HindIII fragment, from the inverse PCR product used to clone the 3′ half of the gene, in pBluescript II SK(−). The final construct, pDAP52, contained a deletion of most of the coding region, including the whole motor domain and part of the tail domain.

The RNA interference (RNAi) *myoB* construct was generated by PCR amplification of the 5′ end of the coding region with primers M13 −21 and myoB3BamHI (5′-AGGATCCCAGCCCTCATCAGTCAGTAG-3′) and cloning into pGEMTeasy (Promega). The resulting plasmid (pDAP31) was digested with BamHI/XbaI, and this fragment was cloned into the green fluorescent protein (GFP) gene-containing pALX196 digested with BglII/XbaI to produce pDAP30. The inducible promoter from the *xylP* gene was removed from pXYLNOM (59) by digestion with EcoRI/NcoI and cloned into pDAP30. The *xylP*(p)::GFP::myoBNt construct was digested with EcoRI/XbaI and cloned into the *pyrG*-containing pALX223 to give pDAP68. The 5′ end of the coding region of *myoB* (myoBNt) was PCR amplified with primers myoB3BamHI and myoBRNAiNcolow (5′-TCCATGGTTGCCGAAGTCGATGAATTGC-3′) and cloned into pGEMTeasy to give pDAP90. The myoBNt fragment from pDAP90 was removed by NcoI digestion and cloned into pDAP68 digested with NcoI, and clones were screened for the proper insert orientation. The resulting plasmid, called pDAP86, contains the RNAi-*myoB* construct under the control of the inducible promoter *xylP*(p) and the selection marker *AnpyrG*.

Fungal strains and media. Strains were grown on *Aspergillus nidulans* medium (ANM) supplemented with 1% or 0.1% glucose as a carbon source and 10 mM γ-aminobutyric acid (GABA) as a nitrogen source at 25°C (15) or on either brain heart infusion (BHI) or synthetic dextrose (SD) medium supplemented with 10 mM $(NH_4)_2SO_4$ as a nitrogen source at 37°C. For induction of constructs under the control of the *xylP* promoter, strains were grown on carbon-free (CF) medium supplemented with 10 mM GABA as a nitrogen source at 25°C or on yeast nitrogen base (YNB) containing 10 mM $(NH_4)_2SO_4$ as a nitrogen source at 37°C and different concentrations of glucose and xylose (15, 59).

The *P. marneffei* FRR2161, SPM4, and $cflA^{D120A}$ strains have been previously described (8). The *myoB* deletion strain (Δ*myoB*::$pyrG^+$) was generated by transformation of SPM4 with the gel-purified deletion construct derived from pDAP52 and selection for $pyrG^+$ transformants. Four transformants showing a distinct growth phenotype were examined by Southern blot analysis, and of these, one strain had a banding pattern consistent with replacement of the wild-type *myoB* allele with the deletion allele with no ectopic copies. Due to the poor aerial growth and the lack of conidia in the Δ*myoB* strain, inoculation of the mutant strain, and of the wild-type strain when it was used as a control, was performed by excising a piece of agar medium containing vegetative growth, disintegrating this, and inoculating into SD liquid medium at 37°C. The liquid culture obtained was then used for inoculation of the corresponding media.

RNAi *myoB* strains were generated by transformation of SPM4 with the plasmid pDAP86 and selection for $pyrG^+$. Transformants were further screened for phenotypes associated with induction on CF medium with 1% xylose.

Microscopy. *P. marneffei* strains were grown on slides covered with a thin layer of solid medium, inoculated with conidia (for RNAi experiments) or vegetative biomass grown at 37°C on SD medium (for deletion mutant experiments) from the appropriate strains, and incubated at the indicated temperature. All slides (except those stained with FM4-64) were fixed in 4% paraformaldehyde for 30 min. Immunofluorescence microscopy for the detection of actin was performed using mouse C4 monoclonal antiactin antibody (Chemicon International) as previously described (10). Plasma membrane staining was performed by immersing slides in 25 μM FM4-64 suspended in water for 15 min at room temperature, washing, and mounting in Tween 80 plus 1 μg μl^{-1} calcofluor white (CAL) as previously described (17, 20). Single-dye control experiments were performed, and these showed no bleeding into the alternative filter set. Slides were examined using differential interference contrast (DIC) and staining with fluorescent brightener 28 (calcofluor white), 4,6-diamidino-2-phenylindole (DAPI), or Hoechst 33342 and visualized on a Reichart Jung Polyvar II microscope. Quantification was performed by counting a 100 cells or septa or 50 conidiophores in three independent experiments. The average number of septa in 100 μm was calculated by recording the number of septa in 10,000 μm in three independent experiments. Images were captured using a SPOT charge-coupled device (CCD) camera (Diagnostic Instruments) and processed in Adobe Photoshop 7.0.

Electron microscopy. Strains were grown on solid ANM for 8 days at 25°C. Excised cubes of agar containing fungal cells were fixed with 1% glutaraldehyde in phosphate-buffered saline (PBS) for 2 h at room temperature and then treated with 1% OsO_4 in PBS for 2 h at room temperature. Samples were slowly

dehydrated on a rotating wheel using increasing concentrations of ethanol (six steps from 10% to 100% and then a repeat 100% step, each for 15 to 20 min). For scanning electron microscopy (SEM), samples were dried in a Balzers CPD 030 critical-point dryer and gold coated in an Edwards S150B gold sputter coater. Samples were examined with a Philips XL30 FEG field emission scanning electron microscope. For transmission electron microscopy (TEM), samples were embedded on a rotating wheel using increasing concentrations of LR white resin (four steps from 25% to 100% and then a repeat 100% step, each for 12 h), and thin sections were examined with a Philips CM120 BioTWIN transmission electron microscope.

Sequence analysis. BLAST searches were performed at the NCBI (http://www.ncbi.nlm.nih.gov/BLAST) (2). Alignments and phylogenetic analyses were performed with ClustalW 1.8 software (http://www.ebi.ac.uk/FTP/index.html). Trees were bootstrapped 1,000 times to assess the reliability of each branch point and drawn using TreeView X. Predictions of coiled-coil regions were performed at MIT (http://groups.csail.mit.edu/cb/paircoil/cgi-bin/paircoil.cgi) (5) and EMBnet (http://www.ch.embnet.org/software/COILS_form.html) (32).

RESULTS

The *P. marneffei* myosin type II homologue. Of the 18 classes of myosins in eukaryotes, four classes (types I, II, V, and XVII) are present in fungi (4). Type II myosins participate in cytokinesis and are important for contraction of the actomyosin ring at the site of division in yeast (13). A fragment of a myosin-encoding gene from *P. marneffei* was cloned by PCR using degenerate primers directed against sequences encoding the motor domain of fungal myosin heavy chains. Sequencing of the PCR fragment and BLAST searches against GenBank revealed high levels of similarity to the motor domains of other myosin heavy chains. This sequence was used to design specific primers that allowed the cloning of the entire gene by inverse PCR, as described in Materials and Methods. The open reading frame spans 7,215 bp and is predicted to have five exons which encode a 2,404-amino-acid protein. The protein shows very high levels of identity to type II myosins in BLAST searches (expect for values of 0.0 with human, *S. cerevisiae*, *S. pombe*, and other type II myosins), and relatedness analysis confirmed that the evolution of fungal type II myosins reflects the evolutionary history of these fungi rather than the different modes of cellular division (see Fig. S1 in the supplemental material). Based on the homology the gene was named *myoB*, following the *A. nidulans* nomenclature, in which the type I myosin was named *myoA* (34).

A search for conserved domains in the MyoB predicted polypeptide sequence using the Pfam databases (http://www.sanger.ac.uk/Software/Pfam/) identified a 680-amino-acid myosin motor domain, which contains a putative ATP binding site, an N-terminal SH3-like fold, and an IQ motif. The coiled-coil prediction algorithms Coils (32) and PAIRCOIL (5) predicted one major coiled-coil region at the N-terminal end of the tail and a second, smaller region toward the C-terminal end, which are separated by regions containing multiple proline residues (see Fig. S2 in the supplemental material). The tails of type II myosins in the filamentous fungi *Aspergillus fumigatus* and *Neurospora crassa* and the yeasts *S. pombe* (Myp2p) and *S. cerevisiae* (Myo1p) also contains several regions with a high probability of forming coiled-coil structures that are separated by proline residues, and this differs from the single coiled-coil region found in *S. pombe* Myo2p and chicken skeletal myosin II (31).

Reverse transcriptase PCR (RT-PCR) analysis showed that *myoB* is expressed during vegetative hyphal growth at 25°C, asexual development at 25°C, and vegetative yeast growth at 37°C (see Fig. S3 in the supplemental material). Expression was slightly higher during asexual development and yeast growth when standardized against expression from the β-tubulin-encoding *benA* gene, presumably reflecting a higher demand for MyoB protein under those conditions. The *myoB* transcript was not detectable by Northern blot analysis (data not shown).

Disruption of *myoB* function. The conventional type II myosin (Myo2) is essential in *S. pombe* (27), as is Myo1p in some genetic backgrounds of *S. cerevisiae* (50). In filamentous fungi vegetative cells do not separate from each other, and we hypothesized that deletion of the type II myosin would not be lethal. A deletion construct in which the entire motor domain and a portion of the tail domain of *myoB* was removed and replaced with the *pyrG*$^+$ selectable marker was generated, and this construct was used to transform *P. marneffei*. PyrG$^+$ transformant strains were screened by Southern blot analysis for replacement of the wild-type gene with the deletion construct and the absence of ectopic copies. Four transformants which showed striking growth defects at 25°C compared to the wild-type strain were isolated, and Southern blot analysis showed that these strains were deleted for *myoB*. One of these strains possessed no additional ectopic copies of the deletion construct and was used for further analysis. The Δ*myoB* strain produced flat colonies (no aerial hyphae) with a waxy appearance and an intense red coloration compared to the wild-type strain (Fig. 1A). Closer examination of the colony also revealed an almost complete absence of mature conidiophores.

At 37°C, the Δ*myoB* strain showed poorer growth on standard defined (synthetic dextrose [SD]) medium than the wild type, and this was partially remediated by high concentrations of osmolytes such as sorbitol or NaCl (Fig. 1B). In contrast, the Δ*myoB* strain was unable to grow on the standard complex undefined (brain heart infusion [BHI]) medium, even in the presence of osmotic stabilizers (Fig. 1B). At 25°C, the deletion strain was able grow on BHI medium (data not shown), suggesting that the growth defects of the Δ*myoB* strain are temperature or cell type specific on this medium. Remediation of growth on defined medium at 37°C by high osmolarity suggested possible cell wall defects in the Δ*myoB* strain. This was tested by growing the mutant and the wild-type strains in defined medium (ANM) containing different concentrations of the cell wall binding agent calcofluor white (CAL) at 25°C. The Δ*myoB* strain showed greater sensitivity to calcofluor than the wild-type strain, supporting the hypothesis of cell wall defects (Fig. 2).

***myoB* is required for correct morphogenesis during hyphal growth.** To investigate the nature of hyphal growth defects in the Δ*myoB* strain, the wild-type and Δ*myoB* strains were grown for 4 or 7 days at 25°C, stained with calcofluor to observe cell walls or with 4,6-diamidino-2-phenylindole (DAPI) for nuclei, and examined microscopically. At 25°C, the wild-type *P. marneffei* grows as septate, branched hyphae which elongate apically. Subapical hyphal cells are predominately uninucleate, whereas apical hyphal cells are multinucleate. After 4 days, only a small number of hyphae from the Δ*myoB* strain exhibited morphological defects such as increased width, aberrant shape, apical branching, and multibranching (2.2% ± 0.2%, compared to 0.7% ± 0.7% for the wild type). However, unlike

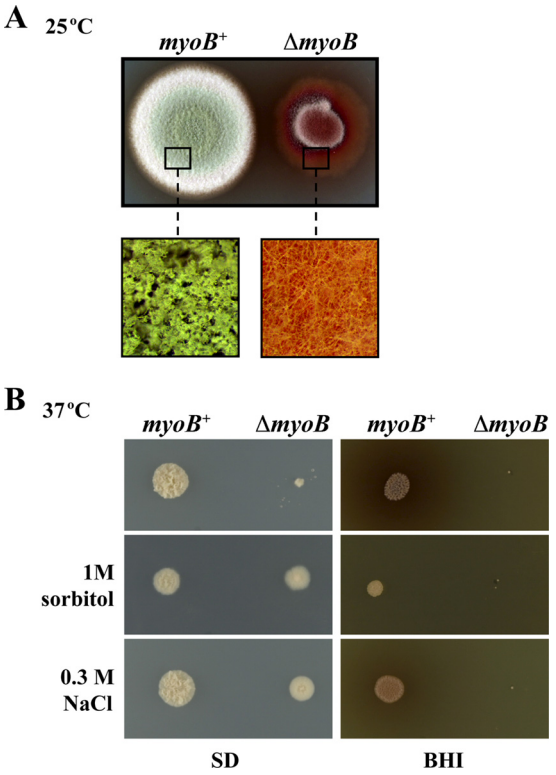

FIG. 1. Deletion of the *myoB* gene leads to growth defects. (A) Deletion of the *myoB* head domain and part of the tail domain by homologous recombination leads to defects in vegetative hyphal growth at 25°C. The wild-type (*myoB*$^+$) and Δ*myoB* strains were grown on ANM for 8 days at 25°C. In comparison to the wild type, the Δ*myoB* strain shows a growth defect (reduced colony diameter) and significantly reduced asexual development (lack of green coloration due to the absence of mature asexual spores). The lower panels show a magnified region of the surface of the colony and the lack of the mature conidiophore structures in the Δ*myoB* strain. (B) Deletion of the Δ*myoB* gene leads to defects in yeast morphogenesis and/or vegetative yeast growth at 37°C. The wild-type (*myoB*$^+$) and Δ*myoB* strains were grown on either SD or BHI medium for 6 days at 37°C with and without the addition of 1 M sorbitol or 0.3 M NaCl as an osmotic stabilizing agent. On SD medium, the Δ*myoB* strain shows significantly slower growth, which is partially remediated by the addition of sorbitol or NaCl. On BHI medium, the Δ*myoB* strain is completely inhibited, and this is cannot be suppressed by the addition of sorbitol or NaCl.

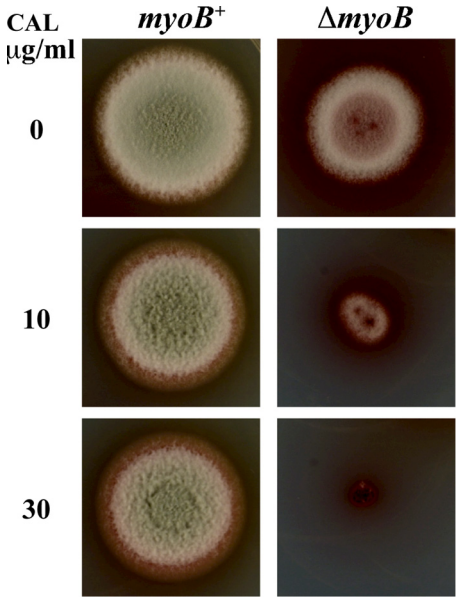

FIG. 2. The Δ*myoB* strain shows increased sensitivity to calcofluor. The wild-type (*myoB*$^+$) and Δ*myoB* strains were grown on ANM for 8 days at 25°C in the presence or absence of different concentrations of the chitin binding agent calcofluor (CAL). The Δ*myoB* strain is significantly more sensitive to calcofluor than the wild type.

for the wild type, hyphae congregated as large longitudinally grouped hyphal bundles which ran along the surface of the agar (Fig. 3A and B; see Fig. S4 in the supplemental material). In contrast, after 7 days at 25°C, 30.1% ± 2.2% of Δ*myoB* hyphae displayed aberrant morphology (compared to 0.7% ± 0.7% for the wild type). Defects ranged in severity across the mycelium and included less severe abnormalities such as thickened and bumpy subapical cells (Fig. 3C and D) and apical cells which were thickened, branched, and occasionally lysed (Fig. 4A) as well as severe defects such as hyphal cell collapse and excessive branching (Fig. 5A and B). Δ*myoB* hyphae also displayed defects in nuclear number, size, and shape, and these defects correlated with morphological defects. The Δ*myoB* hyphae displaying wild-type morphology possessed a low number of aberrant nuclei (6.3% ± 2.5%) compared to the wild type (4.3% ± 2.9%) (Fig. 4B). In contrast, Δ*myoB* hyphae possessing aberrant hyphal morphology had both an elevated number of nuclei (Fig. 4A and 5A) and an increased number of nuclei (46.1% ± 2.9%), which were abnormally shaped and unevenly sized (Fig. 5C).

The phenotype of aberrant, collapsed, and multibranched apical cells is very similar to that previously observed in strains carrying dominant negative alleles of *cflA* (9). *cflA* encodes an orthologue of *S. cerevisiae* Cdc42p which, with the formins Bem1p and Bni1p, participates in a complex set of interactions with the various myosins (types I, II, and V) (23, 29, 57). The *cflA*^{D120A} dominant negative mutants produce hyphae which are swollen and misshapen and which have aberrant, multibranched, and fused apical cells (Fig. 5). However, in contrast to the case for the Δ*myoB* strain, the aberrant apical cells of the *cflA*^{D120A} strain are also multiseptate, and, despite an increase in numbers, nuclear morphology appears to be normal (Fig. 5). This suggests that the Δ*myoB* nucleation phenotype is independent of CflA.

***myoB* is essential for chitin deposition at nascent septation sites.** In *S. cerevisiae*, the type II myosin is required for the formation of the actomyosin contractile ring, which participates in cytokinesis and cell separation (27, 50). Unlike in *S. cerevisiae*, in filamentous fungi cytokinesis (separation of the cytoplasm) is not accompanied by cell separation, but rather the cells remain attached, separated by cross walls called septa. To investigate whether *myoB* is required for septation in *P. marneffei*, septa were examined by calcofluor staining of cell walls in both the wild type and the Δ*myoB* strain after 4 days of growth at 25°C. Wild-type septa occurred at regular intervals along hyphae, with an average of 1.42 ± 0.07 septa per 100 μm (Fig. 3A). In contrast, the Δ*myoB* strain had substantially fewer septa which were unevenly distributed along the hyphae

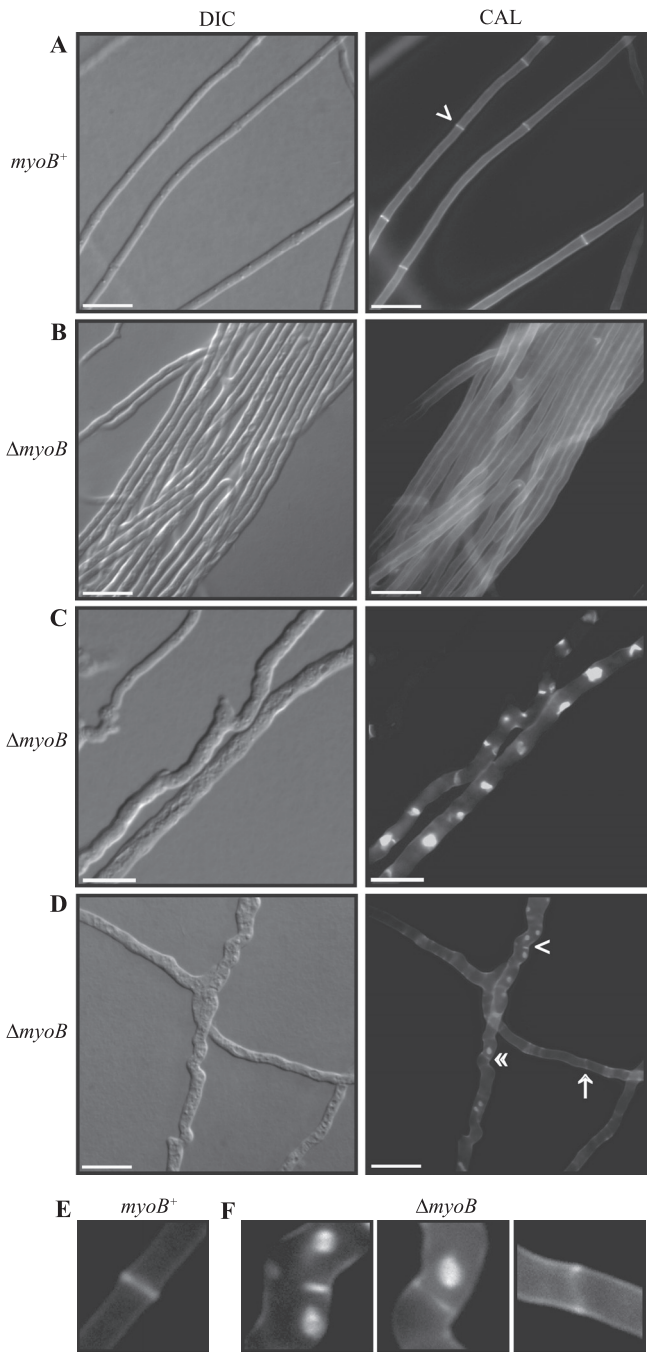

FIG. 3. The Δ*myoB* strain shows defects in chitin deposition. The wild-type (*myoB*$^+$) (A and E) and Δ*myoB* (B to D and F) strains were grown for 4 days at 25°C and stained with calcofluor (CAL) to visualize chitin deposition in cell walls and septa. (A) In the wild type, septa (arrowhead) are observed at regular intervals along hyphae, separating the cellular compartments. (B) In contrast to those of the wild type, the hyphae of the Δ*myoB* strain clump together and form hyphal cables. (C) Large, abnormal deposits of chitin are observed along the hyphae of the Δ*myoB* strain. (D) Aberrant septa are observed in the Δ*myoB* strain. Incompletely formed septa are observed, with chitin on only one side (single arrowhead) or as two separated chitin spots on either side of the hyphae (arrow). Weakly stained complete septa are also observed (double arrowheads). (E) Magnification of the wild-type septum indicated by a single arrowhead in panel A. (F) Magnification of the Δ*myoB* aberrant septa indicated in panel D. Scale bars, 20 μm.

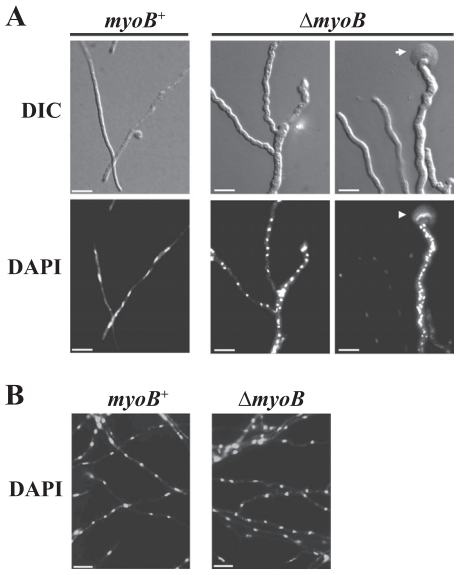

FIG. 4. Aberrant branching and nuclear distribution at the hyphal tips of the Δ*myoB* strain. The wild-type (*myoB*$^+$) and Δ*myoB* strains were grown on ANM for 2 days or 4 days at 25°C and then stained with 4,6-diamidino-2-phenylindole (DAPI) to visualize nuclei. (A) Apical cells of the wild-type (*myoB*$^+$) strain show highly polarized growth without apical branching and regular distribution of nuclei, whereas many apical cells from the Δ*myoB* strain display irregular morphology due to aberrant polarized growth, which is also evident as apical cell branching. In addition, the tips of some apical cells lyse (arrowhead), and these cells contain a large number of DAPI-stained nuclei. (B) Subapical cells from both the *myoB*$^+$ and Δ*myoB* strains often show regular distribution of nuclei despite the lack of normal septation in the Δ*myoB* strain. Scale bars, 20 μm.

(0.10 ± 0.02 septa every 100 μm). In addition, almost all Δ*myoB* septa (95.6% ± 2.0%) appeared very faint, malformed, or absent upon calcofluor staining compared to the wild type (Fig. 3B to F). At a low frequency, some hyphae also showed patches of calcofluor staining, suggesting random or delocalized chitin deposition (Fig. 3C to F).

Transmission electron microscopy (TEM) was performed on the wild-type and Δ*myoB* strains to examine the septation defect. Wild-type septa appeared as a complete and distinct layer separating two cellular compartments in the hyphal cells (Fig. 6). In the Δ*myoB* strain some septa appeared complete; however, many incomplete septa which failed to span the width of the hyphal cell and which displayed a serpentine shape were noted (Fig. 6). This suggests that the *myoB* mutant is partially impaired in the formation of septa.

***myoB* is not required for actin localization at nascent septation sites.** The cortical cytokinetic ring in eukaryotes is composed of actin and myosin. While it has been shown that in fungi such as *S. pombe* and *A. nidulans* cytokinesis is actin dependent, it is also clear that in some fungi, such as *S. cerevisiae*, type II myosins play an important but nonessential role (19, 50). To assess whether actin localization at the septation site is MyoB dependent, actin was visualized by immunofluorescence in both wild-type and Δ*myoB* strains (Fig. 7). In the wild type, both actin and chitin are readily simultaneously detectable at nascent septation sites (Fig. 7A), and this is followed by loss of actin staining in mature septa (10). Surpris-

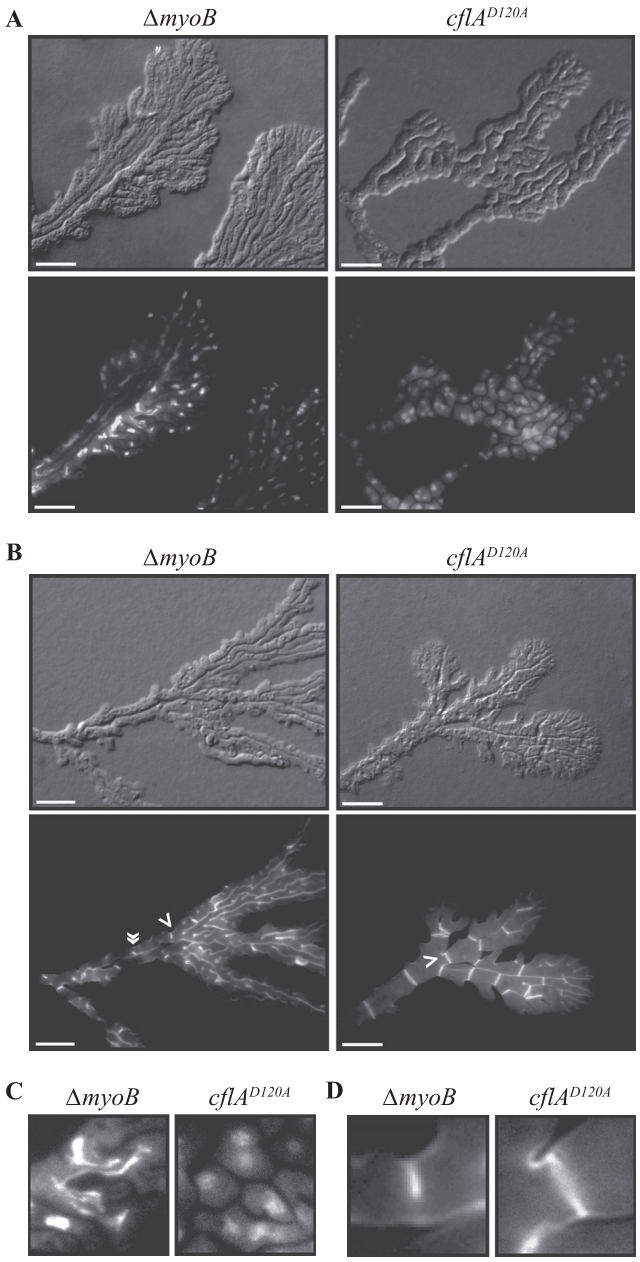

FIG. 5. The Δ*myoB* strain shares phenotypes with the dominant negative *cflA* mutants at 25°C. The Δ*myoB* and *cflA*^{D120A} mutant strains were grown at 25°C on ANM for 7 days and stained with Hoechst 33258 (A and C) or calcofluor (B and D). (A and B) Both the Δ*myoB* and *cflA*^{D120A} mutant strains produce apical cells with aberrant morphology. Apical cells become multibranched and appear fused. (A) In the Δ*myoB* strain, these structures contain nuclei with aberrant morphology, suggestive of nuclear division defects. In contrast, additional nuclei are observed in the *cflA*^{D120A} mutant, and these appear to be normal in morphology. (B) The Δ*myoB* strain has no or aberrant chitin deposition at septal sites. An incomplete septum is indicated by the single arrowhead, and an incomplete septum with a serpentine appearance is indicated by the double arrowheads. In contrast to the case for the Δ*myoB* strain, the aberrant apical cells in the *cflA*^{D120A} mutant have numerous septa. (C) Magnified region from panel A, showing fragmented nuclei in the Δ*myoB* strain compared to nuclei of normal morphology in the *cflA*^{D120A} mutant. (D) Magnified region indicated by the single arrowheads in panel B, showing the incomplete septa formed in the Δ*myoB* strain compared to the formation of normal septa in the *cflA*^{D120A} mutant. Scale bars, 20 μm.

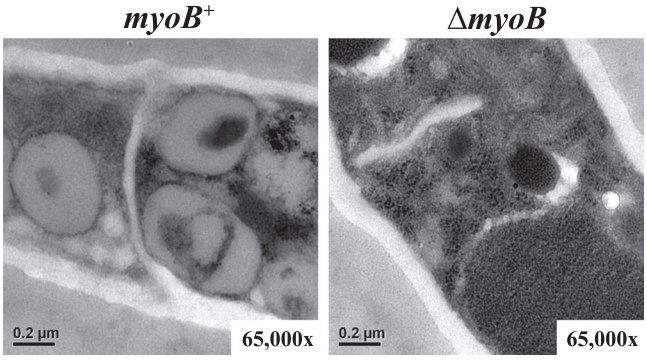

FIG. 6. The Δ*myoB* strain shows incomplete septation. Transmission electron microscopy (TEM) was performed on hyphal cells of the wild-type (*myoB*$^+$) and Δ*myoB* strains grown on ANM for 8 days at 25°C. Comparisons of longitudinal sections show that the Δ*myoB* strain produces incomplete or poorly defined septa compared to the wild-type (*myoB*$^+$) strain.

ingly, actin correctly localized to presumptive septation sites in hyphae of the Δ*myoB* strain, which displayed relatively normal morphology despite the lack of any subsequent chitin deposition and septation (Fig. 7B). In two independent experiments, 100% of the wild-type apical cells with actin staining at nascent septation sites also showed chitin staining ($n = 31$), while 0% of the Δ*myoB* apical cells with actin staining at presumptive septation sites also had chitin staining ($n = 22$). No transverse actin localization, indicative of sites of septation, was observed in Δ*myoB* hyphae which displayed extremely aberrant morphology. Localization of actin at the hyphal apex and cortical actin patches was indistinguishable in the wild-type and Δ*myoB* strains (Fig. 7C and D).

The Δ*myoB* strain is defective in cytokinesis. During cytokinesis, the actomyosin ring contracts, which leads to membrane invagination. The formation of the primary septum separates the two cells and splits the plasma membrane. As the Δ*myoB* strain has normal actin localization at nascent septation sites but lacks chitin at septa, we assessed whether this mutant was capable of cytokinesis during division. The wild type and Δ*myoB* strains were grown for 3 days at 25°C and costained with calcofluor and the lipophilic membrane dye FM4-64 (see Materials and Methods). In the wild type, FM4-64 staining was observed around the cell periphery, surrounding vesicles at the hyphal apex, as a crescent at the presumptive Spitzenkorper, and colocalized with chitin at septation sites as transverse membranes partitioning the hyphae into separate cellular compartments (Fig. 8A). Plasma membrane staining by FM4-64 in the Δ*myoB* strain was also noted at the cell periphery, as vesicles at the hyphal apex, and at the presumptive Spitzenkorper (data not shown). However, in contrast to the case for the wild type, transverse membranes were not readily observed, suggesting that membrane invagination during cytokinesis was defective, thus failing to produce distinct cellular compartments (Fig. 8A). Of the small number of transverse membranes which were observed in the hyphae, some but not all were associated with weakly calcofluor-stained septa. In addition, a large number of circular membranes accumulated along the hyphae of the Δ*myoB* strain (Fig. 8A), and a proportion of these membranes colocalized with the

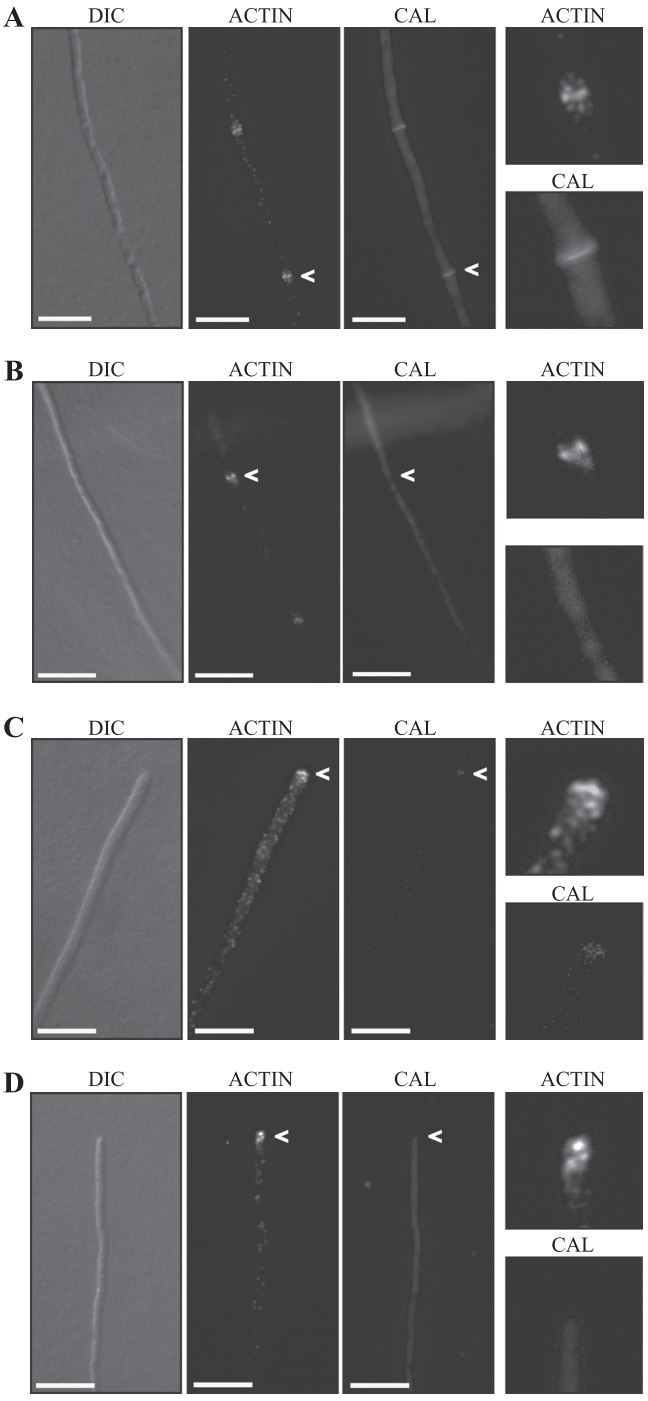

FIG. 7. *myoB* is not required for actin localization at nascent septation sites. The wild-type (*myoB*$^+$) and Δ*myoB* strains were grown on ANM for 4 days at 25°C. Chitin and actin distributions were examined by calcofluor staining (CAL) and immunocytochemistry. Magnified images are shown in the far right panels. (A) In the wild type, actin is localized as cortical actin spots along hyphae and at nascent septation sites (arrowheads). Actin localization at nascent septation sites occurs concomitantly with chitin deposition (arrowheads). (B) Actin is concentrated at nascent septation sites in the Δ*myoB* strain; however, no chitin is deposited at this site. (C) In the wild type, actin is concentrated at the hyphal apex (arrowheads). (D) Actin concentrated at the hyphal apex is also observed in the Δ*myoB* strain. Scale bars, 20 μm.

delocalized chitin spots (Fig. 8B and C). These membranes could be either vesicles or abnormal plasma membrane invaginations.

***myoB* is required for asexual reproduction.** Mature conidiophores were not readily observed on the colony surface of the Δ*myoB* strain (Fig. 1A). To examine this defect further, the wild-type and the Δ*myoB* strains were incubated in defined medium with low (0.1%) glucose (carbon-free [CF] medium), which strongly induces asexual development, for 7 days. These cells were stained with calcofluor to observe cell walls or Hoechst 33258 for nuclei and viewed microscopically. The wild type undergoes asexual development by producing stalks from the vegetative hyphal cells, followed by the differentiation of sterigmata (metula and phialide) cells by sequential budding from the tip of the stalk. Metulae are produced from the stalk and these bud phialides, which in turn repeatedly bud to produce long chains of conidia (asexual spores) (Fig. 9; see Fig. S4 in the supplemental material). All budded cell types of the conidiophore are uninucleate, and each cell type is separated by a septum, reflecting the tight coupling of nuclear division and cell division. Cell-cell adhesion between mature conidia is easily disrupted to liberate free conidia. In contrast to those of the wild type, the conidiophores of the Δ*myoB* strain lacked clearly defined cell types. Typically stalks produced a "phialide-like" cell from which a single terminal conidium was observed. Occasionally one additional malformed phialide-like cell was also noted, which often failed to produce conidia (Fig. 9A; see Fig. S4 in the supplemental material). In the wild type, the conidium-phialide boundary is clearly marked by a septum. Either the conidiophore cells of the Δ*myoB* strain lacked this septum or it was malformed (Fig. 9B). In addition, septa separating the metulae and phialides were also absent or partially formed (Fig. 9A and C). DAPI staining showed that all conidiophores of the Δ*myoB* strain also possessed cells with nuclear abnormalities, and in contrast to the wild type, in which each budded cell type of the conidiophore contains a single nucleus, most of the conidiophore cells (95.7% ± 0.9%) of the Δ*myoB* strain contained nuclei with an aberrant morphology (Fig. 9D). The nuclei appeared fragmented, clumped, and poorly defined, suggesting division defects (Fig. 9D). Unlike the compact nucleus observed in the terminal conidium of the wild type, the nuclei in the terminal conidia of the Δ*myoB* conidiophores were unevenly shaped and string-like (Fig. 9E and F).

***myoB* is required for yeast morphogenesis.** *P. marneffei* is unique among dimorphic fungi in that yeast cells divide by fission rather than budding. In the fission yeast *S. pombe*, which unlike most other fungi has two type II myosins, the *myo2* gene is essential while the *myp2* gene is dispensable (6, 27). Yeast morphogenesis in the wild-type *P. marneffei* is evident after 4 days at 37°C, when cellular division and nuclear division become coupled in cells known as arthroconidiating hyphal cells, and this is followed by the deposition of double septa at sites of cell division and cell separation at these sites to liberate uninucleate yeast cells. This morphogenetic process is termed arthroconidiation, and the resultant yeast cells subsequently divide by fission. Microscopic examination of the Δ*myoB* strain after 4 days at 37°C showed that it cannot undergo arthroconidiation (data not shown). Instead, filamentous growth continues, in which septum staining by calcofluor was hardly dis-

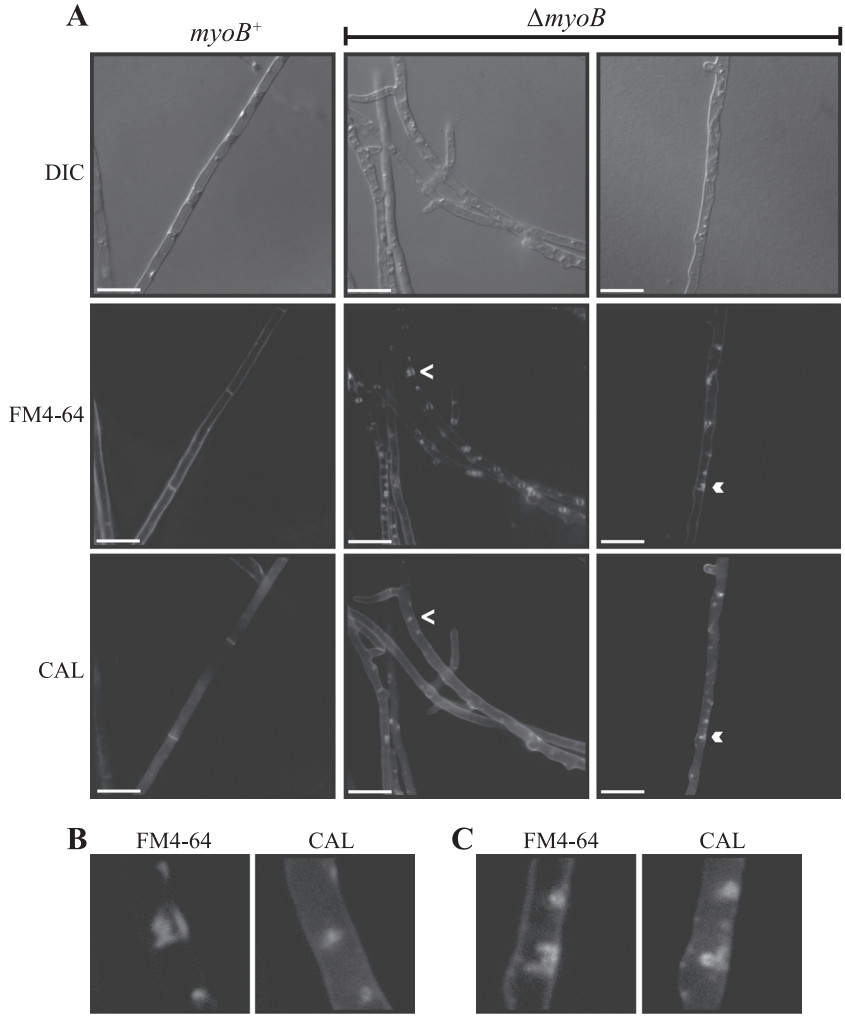

FIG. 8. Distinct cellular compartments are not produced in the Δ*myoB* mutant. The wild-type (*myoB*$^+$) and Δ*myoB* strains were grown on ANM for 3 days at 25°C and costained for calcofluor (CAL) and the membrane dye FM4-64. Single-dye controls showed no background in either channel. (A) In the wild type, the outer plasma membrane and membranes at septation sites are visible. In contrast, the membranes at possible septation sites are not visible in the Δ*myoB* strain; rather, a large accumulation of circular membranes is observed along the hyphae. A proportion of these membranes colocalize with the mislocalized chitin observed in CAL staining (single and double arrowheads). (B and C) Magnification of the regions indicated by the single arrowhead (B) and double arrowhead (C) in panel A, showing colocalization of membranes and chitin in the Δ*myoB* strain. Scale bars, 20 μm.

cernible. The hyphae showed different degrees of branching, and aberrant branching occurred in some apical cells. Similar to the case at 25°C, some cells collapse and show uncontrolled nuclear division. These data suggest that *myoB* type II myosin is important for cell division during yeast morphogenesis and growth in *P. marneffei*.

RNAi targeting of *myoB* recapitulates the phenotypes to the deletion strain. As a consequence of the cellular defects exhibited by the Δ*myoB* strain, it was not possible to genetically complement the mutation. To show that the observed phenotypes are due to loss of *myoB*, an RNAi strategy in which a hairpin construct was under the control of an inducible promoter was adopted (see Fig. S5 in the supplemental material). This SPM4 recipient strain was transformed with the RNAi construct, and transformants were selected for uracil prototrophy (PyrG$^+$) under noninducing conditions. Transfer of the transformants to medium containing increasing concentrations of inducer led to increasing levels of growth inhibition at 25°C (see Fig. S5 in the supplemental material). The strongest phenotype was equivalent to that noted for the deletion strain, namely, an absence of mature conidiophores and a waxy colony appearance with dark red coloration. Microscopic examination of the RNAi *myoB* strains showed wild-type morphology on noninducing medium with septum formation at regular intervals, production of conidiophores under the appropriate conditions at 25°C, and yeast morphogenesis (see Fig. S5 in the supplemental material). Similar to the case for the deletion mutant, when the RNAi strains were incubated in the presence of inducer, very faint or no calcofluor staining of septa was observed. Thus, all of the phenotypes of the deletion strain were recapitulated by the RNAi strains.

DISCUSSION

MyoB is crucial for septum formation. The division of cellular cytoplasm during mitosis (cytokinesis) is an essential pro-

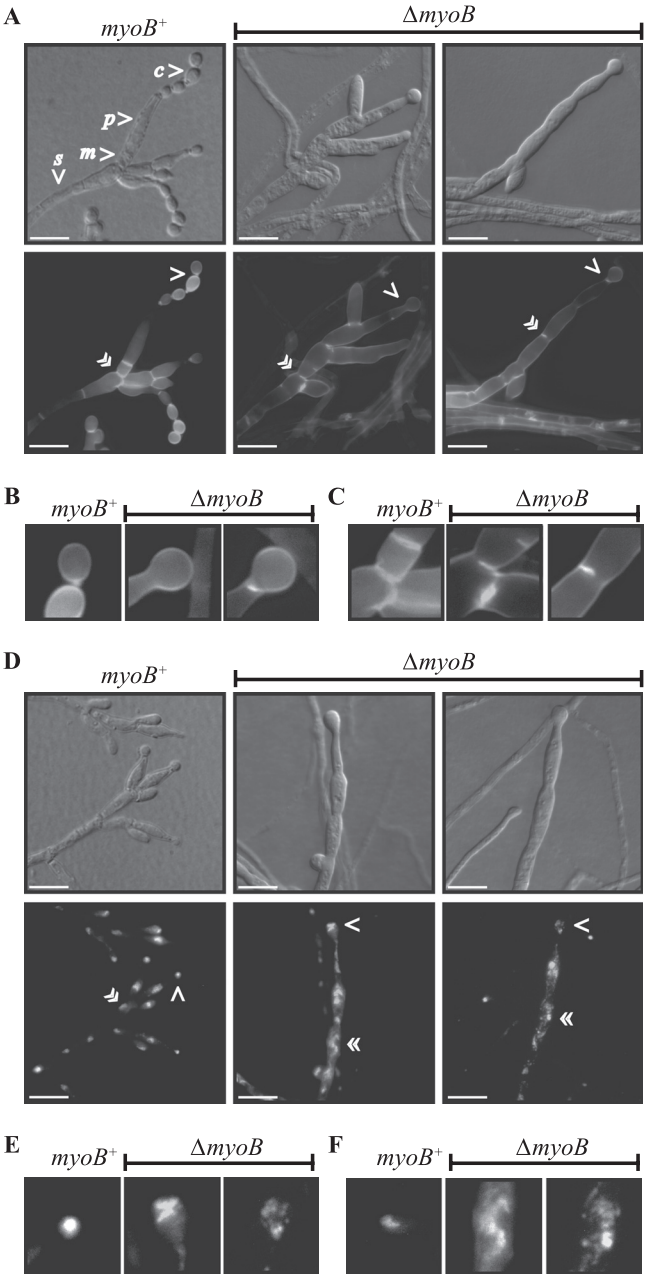

FIG. 9. *myoB* is required for asexual reproduction. The wild-type (*myoB*$^+$) and Δ*myoB* strains were grown on ANM with 0.1% glucose for 7 days at 25°C and stained with calcofluor (CAL) (A to C) or Hoechst 33258 (D to F). (A) Wild-type conidiophores contain a stalk (s) and several metulae (m), phialides (p), and chains of conidia (c). Each cell type is defined by a chitin septal boundary. In contrast, the conidiophores produced by the Δ*myoB* strain have an aberrant morphology and lack clearly defined cell types. A rudimentary conidiophore with one or two phialides and a single terminal conidium is produced. (B) Magnification of the region indicated by single arrowheads in panel A. In the wild type, each conidium is separated by a chitin-containing septum. Some conidiophores of the Δ*myoB* strain completely lack the chitin separation between the phialide and the conidium, whereas others have partially formed septa. (C) Magnification of the region indicated by double arrowheads in panel A. Incomplete septa are observed in the conidiophores of the Δ*myoB* strain. (D) Sterigmata cells of a wild-type conidiophore are uninucleate. Nuclei in the conidiophores of the Δ*myoB* strain showed an aberrant morphology and positioning in the cell, often with a fragmented and stringy appearance indicating division defects. (E) Magnification of the region indicated by single arrowheads in panel D. The nuclei in conidia of the wild type are uniform in shape. In contrast, nuclei in the terminal conidia of the Δ*myoB* strain show aberrant morphology. (F) Magnification of the region indicated by single arrowheads in panel D. The nuclei in phialides of the wild type are uniform in shape. In contrast, nuclei in the phialides of the Δ*myoB* strain show aberrant morphology. Scale bars, 20 μm.

cess during the proliferative growth and development of all organisms. This study has shown that the type II myosin in *P. marneffei*, encoded by *myoB*, is required for the formation of the primary septum during all modes of division. At 25°C, Δ*myoB* hyphae and conidiophores elaborate substantially fewer septa, which are often malformed. Similarly, at 37°C, the arthroconidiating hyphae display very few septa, and consequently no uninucleate yeast cells are produced. Thus, both budding and fission modes of division are affected by deletion of *myoB*. Calcofluor staining showed that chitin was absent from nascent sites of septation and poorly deposited in the few mature septa, which were often incomplete and failed to span the width of the hypha.

Actin localization at nascent septation sites is unaffected in the Δ*myoB* strain despite the deletion strain exhibiting cytokinesis defects and a lack of chitin deposition at these nascent septation sites. This is unexpected, as myosin is essential for actin ring formation in *S. cerevisiae*, *S. pombe*, and *Ashbya gossypii* (7, 25, 31). The simplest explanation is that MyoB is not required for the localization of actin at nascent septation sites in *P. marneffei* but is essential for actin ring contraction during cytokinesis. Another possible explanation for the lack of MyoB-dependent actin ring formation is that *P. marneffei* can use a second, actomyosin-independent pathway to compensate for the loss of *myoB* and allows the formation of actin rings. This may also account for the partially formed and weakly staining septa. In *S. cerevisiae* an independent pathway involving Cyk3p, Hof1p, and Inn1p facilitates actin ring formation and cytokinesis in the absence of Myo1p (7, 22, 28, 44, 52, 53). *P. marneffei* has a conserved Cyk3p homologue (required for actin ring formation), but homologues of either Hof1p (regulates actomyosin ring dynamics and interacts with formins and septins) or Inn1p (required for the ingression of the plasma membrane) are poorly conserved, with BLAST E values of e^{-17} and e^{-5}, respectively (data not shown). It is possible that like in *S. cerevisiae*, the *P. marneffei* Cyk3p homologue allows formation of actin rings in the absence of MyoB; however, unlike in *S. cerevisiae*, cytokinesis cannot proceed due to a lack of Hof1p and Inn1p activity. Searches for homologues of Hof1p and Inn1p in all annotated fungal genome databases showed that they are poorly conserved outside the Saccharomycotina.

Although actin localization is unaffected when *myoB* is deleted, the Δ*myoB* strain lacks chitin deposition at forming septa and accumulates vesicles in hyphae which colocalize with the abnormal chitin deposits. Based on FM4-64 staining, these vesicles are derived from endocytic recycling. It is currently unclear whether the endosomes contain the chitin or are merely located at the same cellular position, which may be locations of failed or incomplete septation. This raises the

possibility that MyoB may be playing a role in the transport of chitin-containing endosomes to the nascent septation sites during cytokinesis. In mammalian cells it has been shown that membrane insertion at the cell center (midbody) is required for abscission of the narrow bridge formed as the cleavage furrow ingresses during cytokinesis (reviewed in reference 37). The membrane vesicles inserted at the midbody are derived from endocytic recycling, but how these endosomes are transported to the midbody remains unclear. The microtubule motor dynein is responsible for endosome clustering during cytokinesis; however, none of the kinesins characterized have been shown to control membrane transport to the bridge (37). This theory is further supported by previous studies which have shown that myosin types V and I are required for transporting vesicles along actin filaments in fungi. Type V myosins are required during exocytosis to deliver secretory vesicles to the growth region in *S. cerevisiae* and to the hyphal apex (and Spitzenkorper) in the plant pathogen *Ustilago maydis* (18, 24, 46, 47). In contrast, type I myosins play a role during endocytosis and have been shown to mediate the endocytic uptake of the marker dye FM4-64 into the vacuole in *A. nidulans* and *Candida albicans* (41, 58). This study suggests that type II myosins may be required for the endocytic transport of vesicles to nascent septation sites during cytokinesis.

Interestingly, the Δ*myoB* mutant displays a phenotype which bears a striking similarity to that of the *A. nidulans* Δ*csmA* mutant. Deletion of *csmA*, which encodes a class V chitin synthase with a myosin motor-like domain (class XVII myosin), results in hyphal lysis and bundling, poorly developed conidiophores, increased sensitivity to calcofluor, and structurally abnormal septa (21). This might indicate either that the vesicles transported to septa by MyoB contain CsmA or that MyoB and CsmA have overlapping roles at the nascent septa.

MyoB-dependent septation is required for developmental progression during conidiation. In contrast to hyphal cells, all cell types of the conidiophore are uninucleate and each cell type is separated by a septum, reflecting a tight coupling of nuclear and cellular division. The Δ*myoB* conidiophores lacked clearly defined cell types and contained multiple nuclei with aberrant morphology. Interestingly, the absence of clearly defined sterigmata cell types may indicate that the sequential production of metulae, phialides, and conidia by budding requires septation to be successfully completed. This hypothesis is further supported by the phenotype of the *P. marneffei* Δ*pakB* strain (*CLA4* homologue) in which although all conidiophore cell types were observed, multiple chains of conidia were not produced due to defects in septation at the phialide-to-conidium cell boundaries (12). Likewise, mutation of the *A. nidulans* septin gene, *aspB*, also resulted in conidiophores which were arrested at the vesicle stage of development (54). The presence of multiple nuclei in the Δ*myoB* conidiophores indicates that lack of septation does not block nuclear division in the *P. marneffei* conidiophore. For *A. nidulans* it is thought that passage through mitosis is required to activate septation (56), and although this is likely to be so for *P. marneffei*, the *myoB* mutation leads to a failure to produce wild-type septa.

The nuclei in the Δ*myoB* conidiophores also appeared clumped. This is likely to be a secondary effect arising from the septation defects exhibited in Δ*myoB* conidiophores. This result suggests that the conidiophore septa may be playing a spatial role in the placement of nuclei in the conidiophore. It is unlikely that MyoB is playing a role in nuclear distribution, as it is generally accepted that microtubules and their associated motors control nuclear migration in filamentous fungi (48). However, there is a small possibility that MyoB may play a role in nuclear positioning in conidiophores, as there is some evidence that in *S. cerevisiae* actin and actin-dependent motors might be required for certain steps in nuclear migration, specifically during the orientation of the spindle pole body (nuclear envelope-embedded microtubule-organizing center), which is required to orient the nucleus with respect to the growth axis of the cell during division (35, 49). This might be crucial during processes which require a switch from a syncytial stage to one with a tight coupling of nuclear and cellular division such as conidiation. In addition, the *S. cerevisiae MYO1* mutant, in addition to displaying an increase in nuclei numbers and a change in morphology, also displays aberrant nuclear positioning during division (7, 53). During division in *S. cerevisiae*, the nucleus has to migrate only a small distance from a random position in the mother cell to the budding neck, where it undergoes mitosis to provide each cell with a nucleus; however, this is clearly a myosin-regulated process.

MyoB clearly does not play an important role during nuclear migration in hyphae. The Δ*myoB* aberrant apical hyphal cells also possessed an elevated number of nuclei, while subapical hyphae with relatively normal morphology showed a normal nuclear distribution, suggesting that MyoB is not required for proper nuclear distribution in hyphae. The elevated numbers of nuclei observed in apical cells are likely to be a secondary effect of disrupting septation due to the mode of duplication in filamentous fungi. In *A. nidulans* nuclear division in apical cells is initiated in waves which extend basally, and this mitotic wave is concluded by septum formation in the apical cell (14, 26, 54). Defects in apical septum formation may result in the loss of the signal to halt the wave of nuclear division.

In summary, this study has shown that the type II myosin in *P. marneffei* is required for the formation of the primary septum in all cell types (vegetative hyphal, yeast, and differentiating conidiophore cells) and modes of division (budding and fission). This indicates that although fungi have evolved different modes of division to suit their life cycle or environment, the molecular mechanisms they utilize have been conserved and are modified to suit the particular application. Understanding how fungi regulate syncytial versus uninucleate growth remains an exciting area for exploration, and filamentous and dimorphic fungi have much to contribute.

ACKNOWLEDGMENTS

We acknowledge Simon Crawford for assistance with the preparation and analysis of samples for electron microscopy and Jenny Greenhalgh for technical assistance.

D.C. was supported by a Marie Curie OIF. K.B. is supported by the National Health and Medical Research Council. A.A. is a Howard Hughes Medical Institute International Research Scholar. This work was supported by grants from the Australian Research Council, National Health and Medical Research Council, and Howard Hughes Medical Institute to A.A.

REFERENCES

1. **Almonacid, M., et al.** 2009. Spatial control of cytokinesis by Cdr2 kinase and Mid1/anillin nuclear export. Curr. Biol. **19:**961–966.

2. **Altschul, S. F., W. Gish, W. Miller, E. W. Myers, and D. J. Lipman.** 1990. Basic local alignment search tool. J. Mol. Biol. **215:**403–410.
3. **Andrianopoulos, A.** 2002. Control of morphogenesis in the human fungal pathogen *Penicillium marneffei*. Int. J. Med. Microbiol. **292:**331–347.
4. **Berg, J. S., B. C. Powell, and R. E. Cheney.** 2001. A millennial myosin census. Mol. Biol. Cell **12:**780–794.
5. **Berger, B., et al.** 1995. Predicting coiled coils by use of pairwise residue correlations. Proc. Natl. Acad. Sci. U. S. A. **92:**8259–8263.
6. **Bezanilla, M., S. L. Forsburg, and T. D. Pollard.** 1997. Identification of a second myosin-II in *Schizosaccharomyces pombe*: Myp2p is conditionally required for cytokinesis. Mol. Biol. Cell **8:**2693–2705.
7. **Bi, E., et al.** 1998. Involvement of an actomyosin contractile ring in *Saccharomyces cerevisiae* cytokinesis. J. Cell Biol. **142:**1301–1312.
8. **Borneman, A. R., M. J. Hynes, and A. Andrianopoulos.** 2001. An STE12 homolog from the asexual, dimorphic fungus *Penicillium marneffei* complements the defect in sexual development of an *Aspergillus nidulans steA* mutant. Genetics **157:**1003–1014.
9. **Boyce, K. J., M. J. Hynes, and A. Andrianopoulos.** 2001. The CDC42 homolog of the dimorphic fungus *Penicillium marneffei* is required for correct cell polarization during growth but not development. J. Bacteriol. **183:**3447–3457.
10. **Boyce, K. J., M. J. Hynes, and A. Andrianopoulos.** 2003. Control of morphogenesis and actin localization by the *Penicillium marneffei* RAC homolog. J. Cell Sci. **116:**1249–1260.
11. **Boyce, K. J., M. J. Hynes, and A. Andrianopoulos.** 2005. The Ras and Rho GTPases genetically interact to co-ordinately regulate cell polarity during development in *Penicillium marneffei*. Mol. Microbiol. **55:**1487–1501.
12. **Boyce, K. J., L. Schreider, and A. Andrianopoulos.** 2009. *In vivo* yeast cell morphogenesis is regulated by a p21-activated kinase in the human pathogen *Penicillium marneffei*. PLoS Pathog. **5:**e1000678.
13. **Brown, S. S.** 1997. Myosins in yeast. Curr. Opin. Cell Biol. **9:**44–48.
14. **Clutterbuck, A. J.** 1970. Synchronous nuclear division and septation in *Aspergillus nidulans*. J. Gen. Microbiol. **60:**133–135.
15. **Cove, D. J.** 1966. The induction and repression of nitrate reductase in the fungus *Aspergillus nidulans*. Biochim. Biophys. Acta **113:**51–56.
16. **Daga, R. R., A. Yonetani, and F. Chang.** 2006. Asymmetric microtubule pushing forces in nuclear centering. Curr. Biol. **16:**1544–1550.
17. **Fischer-Parton, S., et al.** 2000. Confocal microscopy of FM4-64 as a tool for analysing endocytosis and vesicle trafficking in living fungal hyphae. J. Microsc. **198:**246–259.
18. **Govindan, B., R. Bowser, and P. Novick.** 1995. The role of Myo2, a yeast class V myosin, in vesicular transport. J. Cell Biol. **128:**1055–1068.
19. **Harris, S. D., J. L. Morrell, and J. E. Hamer.** 1994. Identification and characterization of *Aspergillus nidulans* mutants defective in cytokinesis. Genetics **136:**517–532.
20. **Hickey, P. C., S. M. Swift, M. G. Roca, and N. D. Read.** 2005. Live-cell imaging of filamentous fungi using vital fluorescent dyes. Methods Microbiol. **34:**63–87.
21. **Horiuchi, H., M. Fujiwara, S. Yamashita, A. Ohta, and M. Takagi.** 1999. Proliferation of intrahyphal hyphae caused by disruption of *csmA*, which encodes a class V chitin synthase with a myosin motor-like domain in *Aspergillus nidulans*. J. Bacteriol. **181:**3721–3729.
22. **Jendretzki, A., I. Ciklic, R. Rodicio, H. P. Schmitz, and J. J. Heinisch.** 2009. Cyk3 acts in actomyosin ring independent cytokinesis by recruiting Inn1 to the yeast bud neck. Mol. Genet. Genomics. **282:**437–451.
23. **Johnson, D. I.** 1999. Cdc42: An essential Rho-type GTPase controlling eukaryotic cell polarity. Microbiol. Mol. Biol. Rev. **63:**54–105.
24. **Johnston, G. C., J. A. Prendergast, and R. A. Singer.** 1991. The *Saccharomyces cerevisiae MYO2* gene encodes an essential myosin for vectorial transport of vesicles. J. Cell Biol. **113:**539–551.
25. **Kaufmann, A., and P. Philippsen.** 2009. Of bars and rings: Hof1-dependent cytokinesis in multiseptated hyphae of *Ashbya gossypii*. Mol. Cell. Biol. **29:**771–783.
26. **King, S. B., and L. J. Alexander.** 1969. Nuclear behaviour, septation, and hyphal growth of *Alternaria solani*. Am. J. Bot. **56:**249–253.
27. **Kitayama, C., A. Sugimoto, and M. Yamamoto.** 1997. Type II myosin heavy chain encoded by the *myo2* gene composes the contractile ring during cytokinesis in *Schizosaccharomyces pombe*. J. Cell Biol. **137:**1309–1319.
28. **Korinek, W. S., et al.** 2000. Cyk3, a novel SH3-domain protein, affects cytokinesis in yeast. Curr. Biol. **10:**947–950.
29. **Lechler, T., A. Shevchenko, and R. Li.** 2000. Direct involvement of yeast type I myosins in Cdc42-dependent actin polymerization. J. Cell Biol. **148:**363–373.
30. **Lippincott, J., and R. Li.** 1998. Sequential assembly of myosin II, an IQGAP-like protein, and filamentous actin to a ring structure involved in budding yeast cytokinesis. J. Cell Biol. **140:**355–366.
31. **Lord, M., E. Laves, and T. D. Pollard.** 2005. Cytokinesis depends on the motor domains of myosin-II in fission yeast but not in budding yeast. Mol. Biol. Cell **16:**5346–5535.
32. **Lupas, A., M. Van Dyke, and J. Stock.** 1991. Predicting coiled coils from protein sequences. Science **252:**1162–1164.
33. **Martin, S. G., and M. Berthelot-Grosjean.** 2009. Polar gradients of the DYRK-family kinase Pom1 couple cell length with the cell cycle. Nature **459:**852–856.
34. **McGoldrick, C. A., C. Gruver, and G. S. May.** 1995. *myoA* of *Aspergillus nidulans* encodes an essential myosin I required for secretion and polarized growth. J. Cell Biol. **128:**577–587.
35. **Miller, R. K., D. Matheos, and M. D. Rose.** 1999. The cortical localization of the microtubule orientation protein, Kar9p, is dependent upon actin and proteins required for polarization. J. Cell Biol. **144:**963–975.
36. **Momany, M., and J. E. Hamer.** 1997. Relationship of actin, microtubules, and crosswall synthesis during septation in *Aspergillus nidulans*. Cell Motil Cytoskeleton **38:**373–384.
37. **Montagnac, G., A. Echard, and P. Chavrier.** 2008. Endocytic traffic in animal cell cytokinesis. Curr. Opin. Cell Biol. **20:**454–461.
38. **Moseley, J. B., A. Mayeux, A. Paoletti, and P. Nurse.** 2009. A spatial gradient coordinates cell size and mitotic entry in fission yeast. Nature **459:**857–860.
39. **Mulvihill, D. P., C. Barretto, and J. S. Hyams.** 2001. Localization of fission yeast type II myosin, Myo2, to the cytokinetic actin ring is regulated by phosphorylation of a C-terminal coiled-coil domain and requires a functional septation initiation network. Mol. Biol. Cell **12:**4044–4053.
40. **Nayak, T., et al.** 2006. A versatile and efficient gene targeting system for *Aspergillus nidulans*. Genetics **172:**1557–1566.
41. **Oberholzer, U., A. Marcil, E. Leberer, D. Y. Thomas, and M. Whiteway.** 2002. Myosin I is required for hypha formation in *Candida albicans*. Eukaryot. Cell **1:**213–228.
42. **Pollard, T. D., and J. Q. Wu.** 2010. Understanding cytokinesis: lessons from fission yeast. Nat. Rev. Mol. Cell Biol. **11:**149–155.
43. **Rajagopalan, S., V. Wachtler, and M. Balasubramanian.** 2003. Cytokinesis in fission yeast: a story of rings, rafts and walls. Trends Genet. **19:**403–408.
44. **Rodriguez, J. R., and B. M. Paterson.** 1990. Yeast myosin heavy chain mutant: maintenance of the cell type specific budding pattern and the normal deposition of chitin and cell wall components requires an intact myosin heavy chain gene. Cell Motil. Cytoskeleton **17:**301–308.
45. **Rose, T. M., et al.** 1998. Consensus-degenerate hybrid oligonucleotide primers for amplification of distantly related sequences. Nucleic Acids Res. **26:**1628–1635.
46. **Schuchardt, I., D. Assmann, E. Thines, C. Schuberth, and G. Steinberg.** 2005. Myosin-V, Kinesin-1, and Kinesin-3 cooperate in hyphal growth of the fungus *Ustilago maydis*. Mol. Biol. Cell **16:**5191–5201.
47. **Steinberg, G.** 2007. Hyphal growth: a tale of motors, lipids, and the Spitzenkorper. Eukaryot. Cell **6:**351–360.
48. **Suelmann, R., and R. Fischer.** 2000. Mitochondrial movement and morphology depend on an intact actin cytoskeleton in *Aspergillus nidulans*. Cell Motil. Cytoskeleton **45:**42–50.
49. **Theesfeld, C. L., J. E. Irazoqui, K. Bloom, and D. J. Lew.** 1999. The role of actin in spindle orientation changes during the *Saccharomyces cerevisiae* cell cycle. J. Cell Biol. **146:**1019–1032.
50. **Tolliday, N., M. Pitcher, and R. Li.** 2003. Direct evidence for a critical role of myosin II in budding yeast cytokinesis and the evolvability of new cytokinetic mechanisms in the absence of myosin II. Mol. Biol. Cell **14:**798–809.
51. **Tran, P. T., L. Marsh, V. Doye, S. Inoue, and F. Chang.** 2001. A mechanism for nuclear positioning in fission yeast based on microtubule pushing. J. Cell Biol. **153:**397–411.
52. **Vallen, E. A., J. Caviston, and E. Bi.** 2000. Roles of Hof1p, Bni1p, Bnr1p, and Myo1p in cytokinesis in *Saccharomyces cerevisiae*. Mol. Biol. Cell **11:**593–611.
53. **Watts, F. Z., G. Shiels, and E. Orr.** 1987. The yeast *MYO1* gene encoding a myosin-like protein required for cell division. EMBO J. **6:**3499–3505.
54. **Westfall, P. J., and M. Momany.** 2002. *Aspergillus nidulans* septin AspB plays pre- and postmitotic roles in septum, branch, and conidiophore development. Mol. Biol. Cell **13:**110–118.
55. **Wolfe, B. A., and K. L. Gould.** 2005. Split decisions: coordinating cytokinesis in yeast. Trends Cell Biol. **15:**10–18.
56. **Wolkow, T. D., S. D. Harris, and J. E. Hamer.** 1996. Cytokinesis in *Aspergillus nidulans* is controlled by cell size, nuclear positioning and mitosis. J. Cell Sci. **109:**2179–2188.
57. **Yakir-Tamang, L., and J. E. Gerst.** 2009. Phosphoinositides, exocytosis and polarity in yeast: all about actin? Trends Cell Biol. **19:**677–684.
58. **Yamashita, R. A., and G. S. May.** 1998. Constitutive activation of endocytosis by mutation of *myoA*, the myosin I gene of *Aspergillus nidulans*. J. Biol. Chem. **273:**14644–14648.
59. **Zadra, I., B. Abt, W. Parson, and H. Haas.** 2000. *xylP* promoter-based expression system and its use for antisense downregulation of the *Penicillium chrysogenum* nitrogen regulator NRE. Appl. Environ. Microbiol. **66:**4810–4816.